JoMathChem manuscript No.
(will be inserted by the editor)

Can We Understand the Branching of Reaction Valleys for more than two Degrees of Freedom?

Wolfgang Quapp

Received: May 7, 2015, accepted: September 7, 2015

Subject area: general interest in theoretical chemistry

Abstract The model of the chemical reaction path is fundamental in Chemistry. We usually understand it as the pathway along a valley of the potential energy surface (PES). However, often a valley bifurcation occurs. This is controlled by a valley-ridge-inflection point (VRI). Up to now, 2-dimensional (2D) figures of a PES govern our understanding. But for more degrees of freedom, this might be misleading. Here, we explain the matter over a 3D configuration space; the PES is then a 3D hypersurface in an R^4. In this case a visualization is possible. We still can project curves on the PES down into the R^3 of the configuration space. A method for the calculation of Newton trajectories (NT) is applied, because NTs bifurcate at VRI points. The example used is a simple mathematical test function. It ends with a threefold combination manifold of three 1D VRI lines. The intersection of the VRI lines forms a super-VRI point. The corresponding singular NT at the super-VRI point has eight branches.

Keywords Valley-ridge-inflection point, VRI manifold, Potential energy surface, Newton trajectory

1 Introduction

PES analysis remains an important basis for classifying and understanding the fundamentals of chemical reactions and their dynamics. It leads to the conception of the so-called minimum energy path, or the reaction path (RP) on a PES [1–3]. The RP is roughly defined as the line which connects two minimizers by passing the saddle point of index one of the PES following the valley in between. The RP is conventionally defined by the mass weighted steepest descent from the saddle point, the intrinsic reaction coordinate(IRC) [4,5]. There are a number of other RP-definitions. The curves which follow projected gradients, named Newton trajectories(NT) can be used. We explain their definition and calculation in Section 2.

NTs open the possibility to find valley-ridge inflection (VRI) points of the PES because NTs bifurcate there. They have branching points (BP). The mathematical description of RP branching is of high interest. In our opinion, it is one of those questions which always requires closer consideration in PES computational chemistry: "The rate of a reaction can be estimated by transition state theory from the

Mathematisches Institut, Universität Leipzig, PF 100920, D-04009 Leipzig, Germany
#E-mail: quapp@uni-leipzig.de, Web: http://www.math.uni-leipzig.de/∼quapp

energy, structure, and vibrational frequencies of the transition state. Reaction path following can identify with some certainty the reactants and products connected by the transition state, unless the path branches. If the branching occurs before the transition state, there will be a separate transition state for each branch, and transition state theory can be used to estimate the relative rates. If the branching occurs after the transition state, ... , the branching ratio cannot be determined by transition state theory, but depends on the nature of the potential energy surface as it descends from the transition state toward the different products. .." [6]

There are a number of older as well as recent studies dealing with aspects of the definition of RPs and their bifurcation: a sizable literature exists concerning BPs [7–10], to name a few. This present paper uses a simple symmetric surface with symmetric VRI points as a model. It is organized as follows: The next section gives a short review to NTs. Section 3 develops the pre-example of a 2D case of the PES used, whereas in Section 4 our explicit goal is to explain the emergence of 1D VRI manifolds for the 3D case of the PES. The last section is a conclusion.

2 Calculation of Newton trajectories

Looking for the potential of the usual RP following to locate bifurcations we have to treat firstly the IRC [4,5]. It is a simple RP concept forming the steepest descent from an SP. This pathway is defined by an autonomous system of differential equations for a tangent vector. Its solution is unique. Therefore, no bifurcation can occur before reaching the next stationary point. Hence, no branching of PES valleys will be truly described by following the IRC, see the discussion in Refs. [11,12] An exception is the symmetric case where we can observe the development of the eigenvalues of the Hessian along the IRC: where their zero is crossed there can be a VRI.

It is helpful to consider that RP branching of NTs is connected with the emergence of a special class of points of the PES, the VRI points [13–15]; we first give a definition of these points.

Definition *A VRI point is that point in the configuration space where, orthogonally to the gradient, at least one main curvature of the PES becomes zero.*
(i) one eigenvalue of the Hessian must be zero, and
(ii) the gradient is orthogonal to the corresponding zero-eigenvector.
VRI points in the sense of the definition exist independently of an RP definition. VRI points are, in general, not identical with BPs of any RP. Usually, VRI points represent non-stationary points of the PES [14]. A problematic aspect of the IRC concept is that the IRC can miss asymmetric VRI points.

We introduced the reduced gradient following [16,15], which is now named Newton trajectory (NT) method. The NT method finds a curve with a selected gradient direction at every curve point [17,18]

$$\mathbf{g}(\mathbf{x})/\|\mathbf{g}(\mathbf{x})\| = \mathbf{r} \ , \tag{1}$$

where $\mathbf{r}$ is the unit vector of the search direction, and $\mathbf{g}$ is the gradient of the PES. Different branches of the solution of the *same* reduced gradient curve in respect to $\mathbf{r}$ may cross each other. Such cross-points of the NT form the VRI points of the surface [15]. Of course, not every NT has such a BP. The path following along those NTs which have a BP allows one to find VRI points – but finding such curves is the general problem. They are named singular NTs, in contrast to the great remainder of regular NTs without a VRI point.

We repeat the way to look for the NTs [16,15,19–21]: we choose a search direction $\mathbf{r}$ being a unit vector and define a projector $\mathbf{P_r}$ which realizes $\mathbf{P_r}\,\mathbf{r} = \mathbf{0}$. It is a constant matrix of rank (N-1) where N

is the dimension of the coordinates. If there is a point $\mathbf{x}$ where the gradient $\mathbf{g}(\mathbf{x})$ fulfills the system of projector equations

$$\mathbf{P_r}\ \mathbf{g}(\mathbf{x})\ = \mathbf{0} \tag{2}$$

then this gradient is named the reduced gradient with respect to the direction $\mathbf{r}$. Solutions of eq.(2) build the NT to direction $\mathbf{r}$. It connects stationary points which differ in their index by one, if no BP is crossed. We numerically follow the curve (2) by tangent continuation. The tangent $\mathbf{x}'$(t) is obtained by the solution of the system of the derivative to the curve parameter

$$\mathbf{0}\ =\ \frac{d}{d\,t}[\mathbf{P_r}\ \mathbf{g}(\mathbf{x}(t))] = \mathbf{P_r}\ \frac{d\,\mathbf{g}(\mathbf{x}(t))}{d\,t} = \mathbf{P_r}\ \mathbf{H}(\mathbf{x}(t))\ \mathbf{x}'(t)\ . \tag{3}$$

$\mathbf{H}$ is the Hessian. In general, the search direction, $\mathbf{r}$, and the tangent, $\mathbf{x}'(t)$, to the NT to $\mathbf{r}$ are different. We use a predictor-corrector method: the predictor step goes along the tangent $\mathbf{x}'$(t), and Newton-Raphson steps of the corrector search (usually orthogonal to this direction) a solution of curve (2) [16, 15,22,21,17,23]. The simplicity of NTs is based on the constance of the $\mathbf{P_r}$ matrix which is used in eq.(3). We recall that NT curves are not generally the so-called valley ground pathways, or valley floor lines. Nevertheless, these curves may follow a valley in favorable cases, at least qualitatively. Like steepest descent curves, also NT curves form a dense family of curves in the coordinate space. Be $\mathbf{g}(\mathbf{x}) \neq \mathbf{0}$ then the point $\mathbf{x}$ is the carrier of an NT to $\mathbf{r}$ where $\mathbf{r} = \mathbf{g}(\mathbf{x})/\|\mathbf{g}(\mathbf{x})\|$.

The early ansatz of Branin [24] to the Newton trajectory method was another one: he uses the adjoint matrix of the Hessian matrix: Branin's NT is defined by

$$\mathbf{x}'(t) = \mathbf{A}(\mathbf{x}(t))\,\mathbf{g}(\mathbf{x}(t))\ , \tag{4}$$

where $\mathbf{A}$ is the adjoint matrix [15] to the Hessian, $\mathbf{H}$. Matrix $\mathbf{A}$ is defined as $((-1)^{i+j} m_{i\,j})^T$ where $m_{i\,j}$ is the minor of $\mathbf{H}$ obtained by deletion of the i^{th} row and the j^{th} column from $\mathbf{H}$, and taking the determinant. The superscript T denotes the transposition. Branin's method is additionally well adapted to exactly calculate symmetric VRI points [15], namely if it is $\mathbf{A}(\mathbf{x})\,\mathbf{g}(\mathbf{x}) = 0$ along an NT.

In the textbook of Jongen, Jonker, and Twilt [25] we find the property of VRI points to build manifolds of dimension $N-2$, if N is the dimension of the PES. We will discuss here the second simplest case (after $N = 2$), the case $N = 3$. Then the VRI points can build a 1D manifold. The existence of a manifold of VRI points is given here not for the first time. A successful search of VRI regions for the molecules H_2O [19], H_2S, H_2Se, H_2CO [20], $C_2H_5^+$ [9], HCN [26,27], and H_5^- [28] is reported. Note that also the approximation of asymmetric VRI points on the PES is a task which was already solved elsewhere [26].

3 A 2D PES model and its VRI points

At the beginning we stated that an RP connects two minima of the PES via a transition state. However, this simple definition does not exclude more complex courses of reactions by a more 'roaming' behavior [29–32]. Such non-RP dynamics may well be the rule rather than the exception for hot molecules. Often the non-RP processes are in regions where a saddle of index two emerges, and we know that between such a summit and the minimum always exits a VRI point.

First we treat the 2D case of a 2D combination of a simple mathematical function ($cos(x)/x^2$ for $2 \leq x \leq 10$) for an explanation. The function can be found in many Calculus text books.

$$E(r_1, r_2) = \sum_{i=1}^{2} \frac{cos(r_i)}{r_i^2} \tag{5}$$

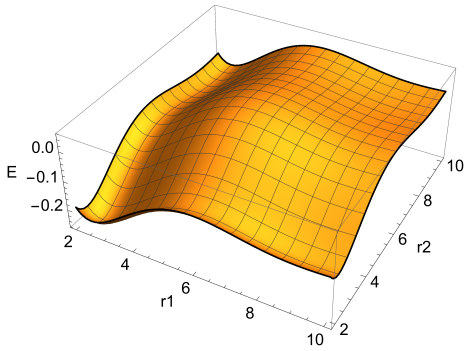

Fig. 1 PES of function (5). One detects four minimums, four saddle points of index one, and one saddle of index two.

In the 2D case we can draw the surface in the 3D space over two coordinates, r_1 and r_2, and one energy coordinate, E, in Fig. 1. Note that we use the two coordinates in a Cartesian manner, and the length unit may be any arbitrary unit. The left global minimum is at $(2.45, 2.45)$, the first SP_1 are at $(5.98, 2.45)$, and $(2.45, 5.98)$, and the next intermediate minimums are at $(9.23, 2.45)$, and $(2.45, 9.23)$. At the symmetry line we have the VRI points at $(3.58, 3.58)$, and $(7.39, 7.39)$, and the summit at $(5.98, 5.98)$.

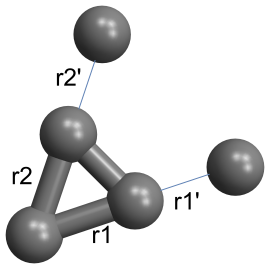

Fig. 2 Three-atomic ring: the extension of bond r_1 for fixed r_2 leads to an SP_1 with distance r_1' to the central atom, as well as the extension of bond r_2 for fixed r_1 leads to a symmetric SP_1 with distance r_2' to the central atom. The symmetric extension first leads to the left VRI point of Fig.3 and then to the SP_2.

A schematic connection to a molecular problem can be seen in Fig.2. (Here the two coordinates would be internal coordinates; nevertheless, we may imagine this molecule in our PES (5). A further reduction of the model is the missing of a third coordinate.) The shown molecular ring may correspond to the global minimum of the PES. A single extension of one bond, r_1 or r_2, is lower in energy than a symmetric double stretching of r_1 and r_2, at the same time. The single extension of one bond leads along a valley up to an SP_1 and after this to a kind of a van der Waals minimum, compare the left panel of Fig.3. At the beginning, the symmetric stretching version also leads uphill in the bowl of the global minimum. But anywhere at the slope the curvature of the level lines changes from convex to concave behavior. The crossing point is the VRI point, see the right panel of Fig.3. A singular NT draws the pathway from minimum to VRI, and from there further uphill to the SP_2. Two unsymmetric branches lead from the VRI point to the two SP_1.

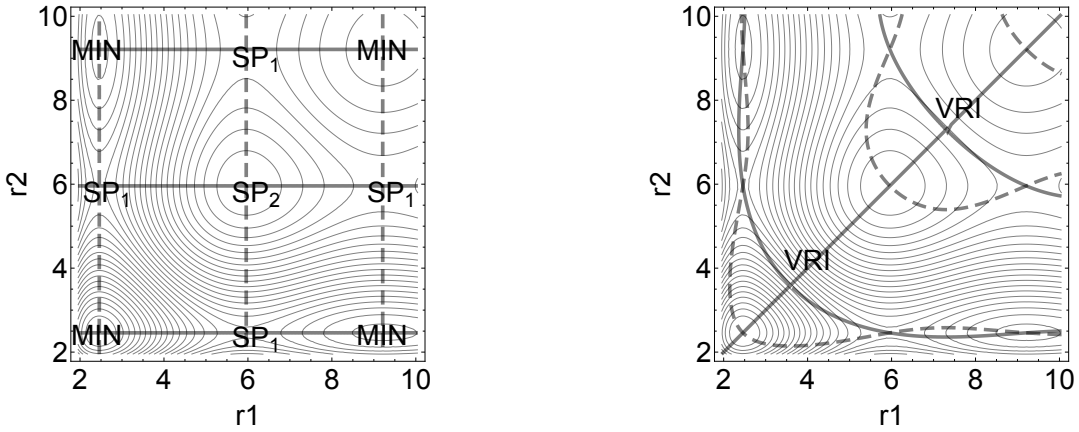

Fig. 3 Level lines of the PES (5) and NTs projected down into the plane of the coordinates, r_1 and r_2. **Left:** NT with full thick lines along direction (1,0), NT with dashes along direction (0,1). They connect the minimums with the SP_1, and these with the SP_2 in the center. The stationary points are nodes of NTs. **Right:** NT with full thick lines along direction (1,1), NT with dashes along direction (1,-1). The singular NT (full line) connects the minimums with the VRI points, and further the VRI points uphill with the SP_2, and with the two corresponding SP_1: a singular NT has four branches.

Note, the surface is 'decoupled' in the sense that there mixed terms do not exist in the definition. Because of this simplicity, the NTs to the coordinate directions, r_1 or r_2, are the valley pathways (the minimum energy paths) or the ridge lines, see Fig.3, the left hand panel.

Another kind of NTs detect the VRI points of the 2D case, see Fig.3, right hand side. They are on the symmetry line r_1=r_2. There the convex region of the corresponding minimum bowl ends, and the concave region of the summit begins, the saddle of index two. We use for the NTs in the case the search directions (1,1) and (1,-1). With the theory of NTs we know that the dimension of the VRI point manifolds on an $N = 2$ dimensional surface is maximally $N - 2 = 0$, thus there only single VRI points can emerge.

4 The 3D PES model and its VRI points

First, we try a kind of training of the imagination by the hypercube, see Fig. 4. We may think the construction of the 4D-cube in the following kind: to every corner of a 3D-cube is added a line of equal length 1 in the forth dimension, so to say, over the 3D configuration space of the 3D-cube is drawn a constant function, a hypersurface of dimension 3, and of value one. In the trivial case of the constant hypersurface, we can it project into the plane: the red 3D-cube. The full region between the former (the black) 3D-cube and the cover hypersurface (the red nodes) is the 4D-cube.

To make the step from the well understandable 2D case of a PES to the not that lucid 3D case of the PES, we extend the former test function by a sum in three degrees of freedom

$$E(r_1, r_2, r_3) = \sum_{i=1}^{3} \frac{cos(r_i)}{r_i^2} \tag{6}$$

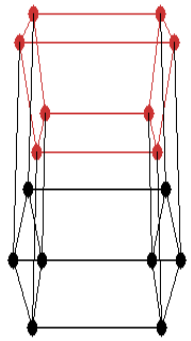

Fig. 4 The black cube is the projection of a normal 3D-cube into a plane. Black and red points together are corners of the 4D-cube, again projected into the plane.

Note that we again use the coordinates r_i in a Cartesian manner. If we use the new r_3 variable at a constant value then we get the former surface (5) plus a constant, thus a 2D problem. (The r_3 coordinate could complete the molecular model of the previous Section 3. To model a trimer, we would have to restrict the coordinates by the triangle inequalities: $r_i + r_j \geq r_k$, for $i, j, k = 1, 2, 3$ and cyclic changes.) Other PES representations for trimers are proposed elsewhere: for T-shaped Ar_3 [33], and for $(LJ)_3$-cluster [22,34,35].

Stationary points on the PES (6) are analogously distributed to the 2D case. Using the symmetry of the PES, we guess the search directions for some series of NTs on the 3D surface, with $r_1 = r_2$ to get the VRI points in this symmetry plane. (We take the search directions as inputs for the NTs and do not discuss here how they are generally chosen.) We generate a sequence of VRI points to different NTs on the PES for different r_3. Figure 5 starts some views to the case of the PES (6).

Because the PES (6) is decoupled, the Hessian has only entries on the diagonal. Then also the adjoint matrix, **A**, has only entries on the diagonal. If we name the second derivatives H_{11}, H_{22}, and H_{33}, then in the simple case we are using here, the entries are A_{11}=H_{22} H_{33}, A_{22}=H_{11} H_{33}, and A_{33}=H_{22} H_{11}. It follows that if $H_{11} = 0$ and if $H_{22} = 0$, on the symmetry plane (r_1=r_2,r_3), one has $\mathbf{A}\,\mathbf{g} = \mathbf{0}$ a VRI point. This happens for a continuity of r_3 sections. Thus, the VRI manifold is a line in the r_1=r_2 plane. The zero curvature happens, for the second derivations, at r_1=r_2=3.58836. The line may start anywhere for values of $r_3 > 2$; realistic molecular values may begin near the global minimum 2.45. A critical value, however, is the threefold symmetric VRI point $r_1 = r_2 = r_3 = 3.58836$. The point is depicted by a red bullet in Figures 5 to 7. It is a 'super'-VRI point because all three second derivatives of the PES are zero there. It should be located in a manifold of dimension $N - 3$, thus zero here. At this 'super'-VRI point ends the 3D valley of the global minimum, and the 3D ridge of the SP_3 begins. It is the meeting point of the former VRI line with the two other VRI lines in the planes (r_2=r_3,r_1) and (r_1=r_3,r_2), see Fig. 7. The family of singular NTs through the VRI line in Figures 5 and 6 concerns the symmetry plane (r_1=r_2,r_3). Two other analogous families of singular NTs exist in the symmetry planes (r_1=r_3,r_2) and (r_2=r_3,r_1). We sketch the situation in Fig. 7 where only some outer NTs of the corresponding families are drawn. It is a symmetric picture. Every one of the singular NTs of Fig. 7 (thick black bullets) corresponds to the singular NT of Fig. 3, right panel. The lower one in Fig. 7 is the NT with r_3 fixed to the global minimum value of 2.45, thus, it is an NT from the 2D problem. Analo-

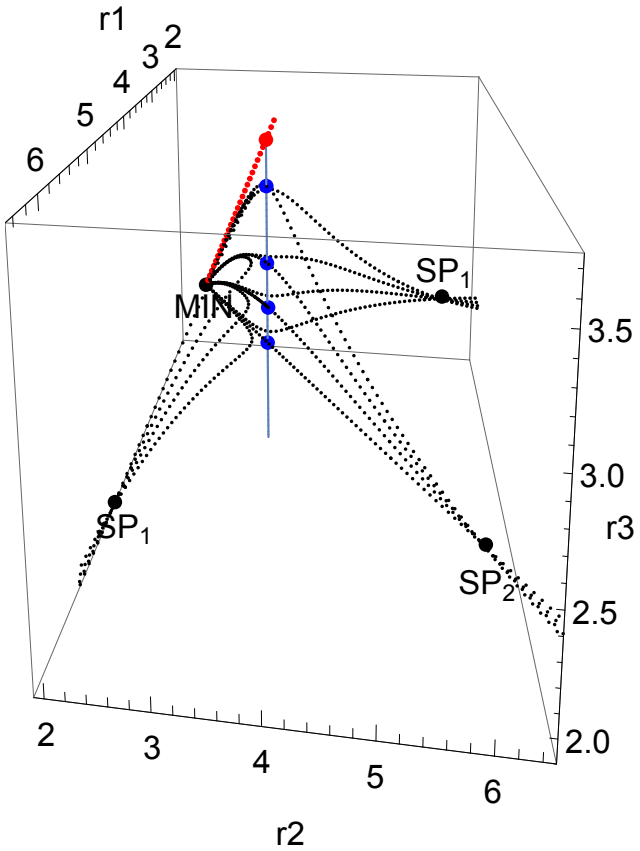

Fig. 5 Projections of NTs on the PES (6) down into the coordinate space by dotted curves. Four singular NTs from MIN to SP_2 go through VRI points (blue bullets) in the symmetry plane (r_1=r_2, r_3). To every singular NT two accompanying regular NTs are given which connect the MIN with the two symmetric SP_1 in the corresponding (r_1, r_3), or (r_2, r_3) planes. The diagonal red line is the fully symmetric NT. The red VRI point is a super-VRI, see text. The blue line is a line of VRI points from the super VRI to the bottom of the figure: it is a part of the VRI-manifold.

gously, the left NT is drawn for fixed r_2=2.45, and the last one at the back side is drawn for fixed r_1=2.45.

The VRI points in the plane (r_1=r_2,r_3) form a straight line. Depending on the parameter, r_3, we find different energies along this line. We show the relation in Fig. 8.

Not shown in Fig. 7 is that the VRI manifold (the three blue straight lines) continues 'above' the super VRI. However, the character of its VRI points changes. Below the super VRI the branches of a singulat NT either connect the minimum and an SP_2, or the two SP_1 'left and right' from the corresponding symmetry plane. Above the super VRI the 4 branches of a singular NT through a VRI point now connect either two SP_2, or they connect the SP_1 in between and the SP_3, correspondingly. Note that again the index theorem for NTs [36] holds.

From the chemical point of view for a trimer, the 'upper' region of the VRI manifold is not so interesting, because the energy values are high. They are very higher than the energies of the reaction pathways over the SP_1. The encounter of the two regions of the VRI manifold is the super VRI point.

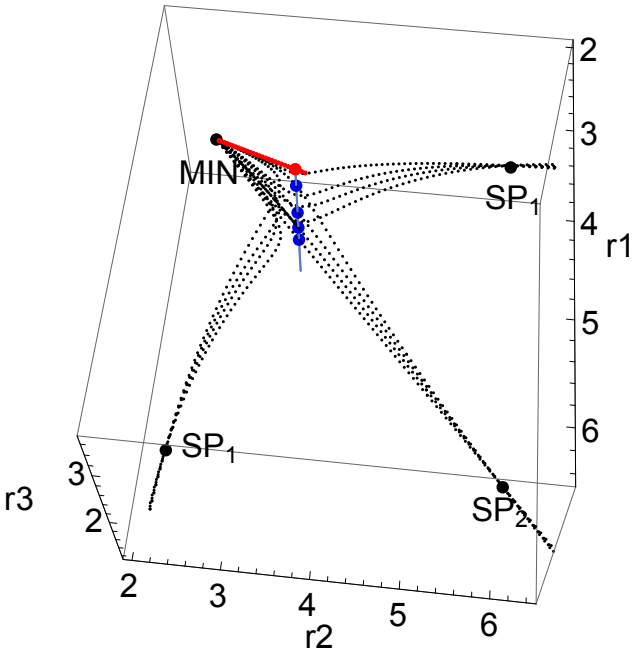

Fig. 6 Same as Fig.5. The viewpoint is from above. Compare the 2D case in Fig. 3, right panel. It seems to be the perpendicular projection of the 3D case.

Here, the singular branches unite of the VRI points of the two different parts of the VRI manifold. The singular 'super' NT through the super VRI has 8 branches: the two fully symmetric lines to minimum and to SP_3 (the lines of red bullets), the three branches to the three SP_2, and the three branches to the three SP_1, compare Fig. 7.

5 Conclusion

By Fig. 9 we discuss our result: the VRI points form a manifold in the configuration space of the molecule where the corresponding point of the manifold depends on the distance r_3. This r_3 is a parameter, or an spectator variable for the bifurcation occurrence of the corresponding NT. Here, with the uncoupled PES (6), we find the VRI point for the same values (r_1,r_2)=(3.58836,3.58836), for every value r_3 of a certain interval. In a realistic molecular PES, we will find curvilinear manifolds of VRI points for changing values of the parameter [19,20,9,26–28]. The critical bound for r_3 is here the symmetry case r_1=r_2=r_3 = 3.58836 where at the crossing of the three zero eigenvalues on the symmetric NT the super VRI emerges: the red bullet in Fig. 7.

An energetically global, lower VRI point emerges if r_3 has the equilibrium value of the global minimum, or r_1 or r_2 are at their lower minimums, respectively. The corresponding points are the three blue bullets in Fig. 7. For shorter r_3 a compression of the remaining diatom leads again to a higher energy. If the remaining diatom in Fig. 9 vibrates [37], this can happen. But the shortening of the bond has physically quickly an end. Thus, the VRI manifold should be continuable behind the fat black NTs in Fig. 7, however, not very wide.

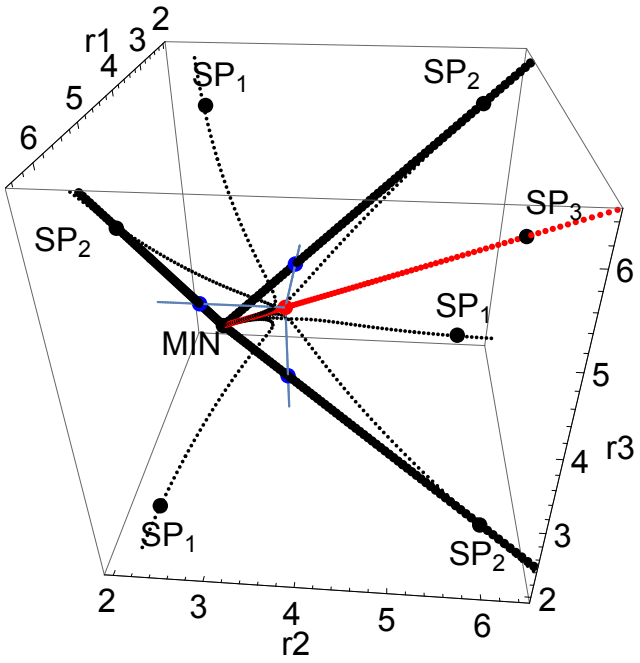

Fig. 7 Projections of NTs on the PES (6) into the coordinate space. Shown is the threefold symmetry of the PES. Three 'outer', straight singular NTs (black bullets) connect the MIN with the three SP_2. Three regular NTs (thin black points) are shown which connect the MIN with the three SP_1 but touch the VRI region, as well as three further singular NTs are shown (also thin black points) which connect the MIN over a VRI (near the super VRI, red bullet) with the three SP_2. The last NTs cross the VRI manifold (light blue line). Three parts of the VRI manifolds are depicted in light blue where the red line is the fully symmetric NT from MIN to SP_3.

One should compare this example (6) of this paper with the older, somewhat more difficult case of Ref. [15] where also a 3D test PES is treated.

The index theorem for NTs [36] is coupled with the manifold character of the VRIs for Newton trajectories. It is similar to the Mezey-partitioning for steepest descent curves into catchment regions [38–41]. There the borders are formed by (N-1)-dimensional ridges starting from the SPs of index one. Here the borders are formed by the one-dimensional singular NTs starting at the (N-2)-dimensional manifold of VRI points. Together this set of points again forms an (N-1)-dimensional partitioning of the coordinate space.

As the name suggests, stationary points are true, singular points on the PES. The condition is that the gradient is the zero vector. (We do not treat the exception of a degenerate surface.) One can try to imagine such points also on a higher dimensional PES, especially the orthogonal dynamics to the SP col [42]. However, we have learned here that VRI points are usually parts of a larger manifold. Their main property (zero eigenvalue(s) of the Hessian) is not concentrated on an isolated point. We face an unforeseen challenge which such simple molecules, beginning with trimers, hold for our understanding. If we start in a minimum and go uphill in the direction to a ridge, then we usually meet not just one VRI point, where the bowl valley bifurcates. For a continuity of values of a parameter variable, or more parameter variables in still larger molecules (spectator variables), we find different VRI points. But the good news is: for (a) fixed value of the parameter(s) we have exactly one VRI point. In our simple

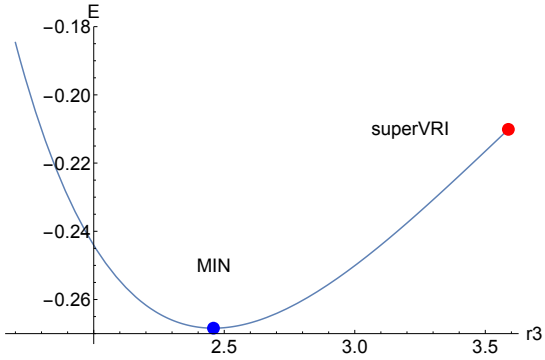

Fig. 8 PES section over the (r_1=r_2,r_3) plane for the VRI line. The symmetric value of bonds r_1 and r_2 is fixed at (3.58836, 3.58836), where the 'parameter', r_3, can vary. The PES varies with it. Because of the simplicity of the PES, one can compare an analogous energy curve at the edges of Fig. 1, but only somewhat lifted.

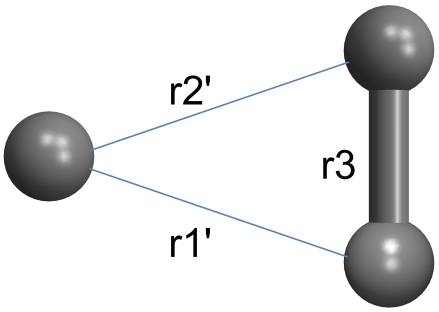

Fig. 9 Escape of one atom from the three-atomic ring: the symmetric extension of bonds r_1 and r_2 leds up to a VRI point on the PES with distances r_1' and r_2' to the remaining diatom. This happens for an aggregate interval of r_3 values.

example we have three energetically lowest VRIs, and at the other end there is one super VRI which is also energetically maximal, see Fig. 8. Such border VRIs may build a frame for our understanding.

Acknowledgment
I thank Prof. J.M. Bofill (Barcelona) for the (last) impulse to this paper.

References

1. K. Laidler, *Theory of Reaction Rates* (McGraw-Hill, New York, 1969)
2. D. Heidrich, W. Kliesch, W. Quapp, *Properties of Chemically Interesting Potential Energy Surfaces* (Springer, Berlin Heidelberg, 1991)
3. D. Heidrich (ed.), *The Reaktion Path in Chemistry: Current Approaches and Perspektives* (Kluwer Academic Publishers, Dordrecht, 1995)
4. K. Fukui, J. Phys. Chem. **74**, 4161 (1970)
5. W. Quapp, D. Heidrich, Theor. Chim. Acta **66**, 245 (1984)
6. V. Bakken, D. Danovich, S. Shaik, H.B. Schlegel, J. Am. Chem. Soc. **123**, 130 (2001)
7. W. Quapp, Theoret. Chim. Acta **75**, 447 (1989)
8. J.Q. Sun, K. Ruedenberg, J. Chem. Phys. **100**, 5836 (1994)

9. W. Quapp, D. Heidrich, J. Molec. Struct. THEOCHEM **585**, 105 (2002)
10. W. Quapp, J. Molec. Struct. **695–696**, 95 (2004)
11. H.B. Schlegel, J. Chem. Soc., Faraday Trans. **90**, 1569 (1994)
12. W. Quapp, J. Chem. Soc., Faraday Trans. **90**, 1607 (1994)
13. H. Metiu, J. Ross, R. Silbey, T.F. George, J. Chem. Phys. **61**, 3200 (1974)
14. P. Valtazanos, K. Ruedenberg, Theor. Chim. Acta **69**, 281 (1986)
15. W. Quapp, M. Hirsch, D. Heidrich, Theor. Chem. Acc. **100**, 285 (1998)
16. W. Quapp, M. Hirsch, O. Imig, D. Heidrich, J. Comput. Chem. **19**, 1087 (1998)
17. M. Hirsch, W. Quapp, J. Comput. Chem. **23**, 887 (2002)
18. W. Quapp, J. Theoret. Comput. Chem. **2**, 385 (2003)
19. M. Hirsch, W. Quapp, D. Heidrich, Phys. Chem. Chem. Phys. **1**, 5291 (1999)
20. W. Quapp, V. Melnikov, Phys. Chem. Chem. Phys. **3**, 2735 (2001)
21. W. Quapp, Optimization **52**, 317 (2003)
22. W. Quapp, M. Hirsch, D. Heidrich, Theor. Chem. Acc. **105**, 145 (2000)
23. E.L. Allgower, K. Georg, *Numerical Continuation Methods - An Introduction* (Springer, Berlin, 1990)
24. F.H. Branin, IBM J. Res. Develop. **16**, 504 (1972)
25. H. Jongen, P. Jonker, F. Twilt, *Nonlinear Optimization in Finite Dimensions* (Kluwer Academic Publ., Dordrecht Boston London, 2000)
26. W. Quapp, B. Schmidt, Theor. Chem. Acc. **128**, 47 (2011)
27. B. Schmidt, W. Quapp, Theor. Chem. Acc. **132**, 1305 (2012)
28. R.M. Minyaev, W. Quapp, B. Schmidt, I.V. Getmanski, V.V. Koval, Chem. Phys. **425**, 170 (2013)
29. A.E. Pomerantz, J.P. Camden, A.S. Chiou, F. Ausfelder, N. Chawla, W.L. Hase, R.N. Zare, J. Am. Chem. Soc. **127**, 16368 (2005)
30. A.G. Suits, Acc. Chem. Res. **41**, 873 (2008)
31. B.R. Heazlewood, M.J.T. Jordan, S.H. Kable, T.M. Selby, D.L. Osborn, B.C. Shepler, B.J. Braams, J.M. Bowman, Proc. Natl. Acad. Sci. USA **105**, 12719 (2008)
32. Z. Lu, Y.C. Chang, Q.Z. Yin, C.Y. Ng, W.M. Jackson, Science **346**, 61 (2014)
33. R. Guantes, A. Nezis, S.C. Farantos, J. Chem. Phys. **111**, 10836 (1999)
34. R.J. Hinde, R.S. Berry, D.J. Wales, J. Chem. Phys. **96**, 1376 (1992)
35. L.L. Lohr, Mol. Phys. **97**, 977 (1999)
36. M. Hirsch, W. Quapp, J. Molec. Struct., THEOCHEM **683**(1–3), 1 (2004)
37. W. Quapp, B.P. Winnewisser, J. Math. Chem. **14**, 259 (1993)
38. A. Tachibana, K. Fukui, Theor. Chem. Acc. **51**, 189 (1979)
39. P. Mezey, Theor. Chem. Acc. **58**, 309 (1981)
40. P. Mezey, *Potential Energy Hypersurfaces* (Elsevier, Amsterdam, 1987)
41. P. Mezey, Theor. Chem. Acc. **102**, 279 (1999)
42. F.A. Mauguière, P. Collins, G.S. Ezra, S. Wiggins, Int. J. Bif. Chaos **23**, 1330043 (2013)